EJB Electronic Journal of Biotechnology ISSN: 0717-3458
Vol.2 No.3, Issue of December 15, 1999.

Received August 20, 1999 / Accepted October 18, 1999.

RESEARCH ARTICLE

Visualization and Functional Analysis of a Maxi-K Channel (*mSlo*) Fused to Green Fluorescent Protein (GFP)

Michael P. Myers *
Department of Pharmacology and Physiology
University of Rochester School of Medicine and Dentistry,
Rochester, New York, USA 14642-8711.
E-mail : adric@ucla.edu

Jay Yang
Department of Pharmacology and Physiology, and Department of Anesthesiology
University of Rochester School of Medicine and Dentistry,
Rochester, New York, USA 14642-8711.
E-mail : jyang@anes.rochester.edu

Per Stampe
Department of Pharmacology and Physiology
University of Rochester School of Medicine and Dentistry,
Rochester, New York, USA 14642-8711.
E-mail : ps@crocus.medicine.rochester.edu

We have constructed a fusion protein between *mSlo* (a recombinant, high conductance, calcium-activated potassium channel or maxi-K), and GFP (green fluorescent protein). This construct represents a tag to not only monitor channel expression, but to locate the protein in living cells. The GFP was fused in frame to the carboxy-terminus of the *mSlo* core protein (*mSlo*-GFP fusion protein). Expression of this fusion protein in COS-7 cells resulted in robust fluorescence localized near the cell membrane. Fluorescing cells that were patch clamped exhibited whole cell currents with a direction consistent with potassium currents. Conversely, non-fluorescing cells showed no significant whole cell currents. Excised inside out patches revealed single channel currents and calculated conductances in the range of those expected for the maxi-K. The *mSlo* and *mSlo*-GFP channels reconstituted into lipid bilayers bound wild-type, recombinant CTX with high affinity and displayed a half-blocking concentration (K_D) of 7.4 and 7.6 nM, respectively (at +30 mV in 150 mM equimolar KCl). This resulted in single channel evaluation of the functional inhibition of CTX on these clones. As newly constructed GFP chimeras emerge for the study of physiological processes in living organisms, this work provides another area of insight illuminated by GFP.

Green Fluorescent Protein (GFP), cloned from the jellyfish *Aequorea victoria* is a powerful tool for biotechnology in studying the expression of various proteins. GFP is easily visualized when excited with UV light and its fluorescence does not depend on any exogenous compounds (Marshall et al., 1995). This protein, when expressed alone, appears cytosolic, with no cellular targeting mechanisms of its own, making it ideal to tag a protein of interest. Our fusion construct, called *mSlo*-GFP (for a review of GFP nomenclature see Gerdes and Kaether, (1996)), has the green fluorescent protein fused in frame to the c-terminus of the channel. The result is a functional tagged potassium channel. Our results demonstrate that the fusion protein can be expressed in COS-7 cells, harvested, and reconstituted into lipid bilayers allowing detailed single channel analysis. In addition, we show that the fusion protein can be studied by patch clamp techniques as well.

Maxi-K channels belong to a class of calcium sensitive potassium channels which possess a large single channel conductance (greater than ~ 200 pS in symmetrical 150 mM KCl), thus they have been called BK (big potassium) or maxi-K channels (Latorre et al., 1989). These high conductance channels have been measured in numerous tissues and are associated with various physiological processes, including the repolarization of action potentials in neurons, regulation of fluid secretion in exocrine cells, and maintenance of contractile tone in smooth muscle (McManus, 1991). Recent physiological work has linked maxi-K channels to the mediation of vasorelaxant effects of K^+ channel openers in the porcine coronary artery

*Corresponding author

(Balwierczak et al., 1995), to the regulation of airway cholinergic neurotransmission (Tagaya et al., 1995), to the control of the dynamics ofaqueous humor outflow in the anterior of the human eye (Stumpff et al., 1997), and to second messenger systems contributing to the membrane conductance of retinal Müller cells (Bringmann et al., 1997). These large conductance channels have also been implicated in several diseases, including the pathogenesis of hypertension in spontaneously hypertensive rats (Asano et al., 1995), the molecular mechanism of antiasthma therapy (Barnes, 1995), and to the inherited susceptibility to non-insulin-dependent diabetes mellitus (NIDDM) (Ferrer et al., 1996).

While a great deal of information has been accumulated from studying native maxi-K channels, the channel was difficult to clone and then to express. This has barred it from the explosion of data provided by molecular biology that has increased our knowledge of other potassium channels. Maxi-K channels have been cloned and expressed from the *slowpoke* locus (Adelman et al., 1992). This began the molecular characterization of the channel. The first maxi-K mammalian clone from the mouse brain (*mSlo*) appeared in 1993 (Butler et al., 1993). Human analogues (*hSlo*) of this channel have been cloned from a variety of sources including the brain (Dworetzky et al., 1994; Tseng-Crank et al., 1994), arterial smooth muscle (McCobb et al., 1995), myometrium (Wallner et al., 1995), and pancreatic islet cells (Ferrer et al., 1996). While structurally homologous to the purely voltage-gated potassium channels such as *Shaker* (both are characterized by six n-terminus hydrophobic membrane spanning domains and an additional pore domain), the cloned DNA for maxi-K channels is more than double the size, containing a large c-terminus coding region believed to confer their calcium sensitivity (Knaus et al., 1995; McCobb et al., 1995; Adelman et al., 1992). This increased size may be one reason that causes the difficulty of channel expression. Cloned maxi-K channels appear to express well in *oocytes*, yielding robust macropatch cell currents, but single channel analysis necessary for detailed kinetic analysis of CTX block has not been forthcoming, especially in the mammalian clones (Butler et al., 1993; McCobb et al., 1995). Furthermore, studies measuring the affinity of CTX to BK channels reconstituted into artificial bilayers such as the one described here, have an advantage in that oocytes as an alternative expression system are now known to be contaminated with native BK channels (Krause et al., 1996). The initial characterization of the pharmacology of cloned maxi-K channels was completed only recently (Gribkoff et al., 1996), and our work adds to the analysis of the *mSlo* clone, particularly with regard to its interaction with CTX.

CTX has been very useful in studies of ion channel structure and function. Its interaction with specific residues in the pore region of ion channels makes it an ideal probe when relating specific amino acids to their physiological role. Studies show CTX to be 37 amino acids in length, 20 x 20 x 25 Angstroms in dimension, with a globular structure formed by a three-turn alpha helix lying on an antiparallel β sheet with three internal disulfide bonds (Bontems et al., 1991). Use of CTX has not only identified residues in contact with the toxin, it marks residues in proximity to the receptor for CTX (Goldstein et al., 1994). When CTX is applied to preparations of native maxi-K channels, it blocks the channel in a bimolecular fashion, binding to the external vestibule of the channel and physically occluding or "plugging" the outer entry to the conduction pore (Miller, 1995). Moreover, studies of CTX binding have linked specific residues on the toxin to permeation sites in the pore, enriching our molecular picture of the toxin and the nature of its receptor in potassium channels (Naini et al., 1996). Recently, CTX and its close scorpion toxin analogue, agitoxin2, have been used to show that prokaryotic K^+ channels have the same pore structure as eukaryotic K^+ channels (MacKinnon et al., 1998). This result is important, given that the crystal structure of a prokaryotic K^+ channel from *Streptomyces lividans* has been revealed by Doyle et al. (1998). The testing of this ground-breaking structure will require detailed toxin profiles, such as those presented here, especially if we are to extrapolate the structure of a two-transmembrane K^+ channel to a six-transmembrane K^+ channel, such as *Shaker*, or to an even more complex ten-transmembrane K^+ channel, such as the maxi-K described in this report. Preliminary data of these findings have been reported in abstract form (Myers et al., 1997).

Materials and Methods

Molecular biology

For the expression of GFP alone, Green Fluorescent Protein cDNA (from the pGFP clone, Clontech, Palo Alto, CA) was subcloned into expression vector pMT3 (from the laboratory of Daniel D. Oprian, Brandeis University). The pMT3 vector is pMT2 (Sambrook et al., 1989) with the Pst I and Eco RI sites mutated to Kpn I and Not I, respectively. To express GFP as a fusion protein, the GFP was subcloned into an expression vector of pMT3 containing the α subunit of *mSlo* (mbr5) (Butler et al., 1993). The stop codon in *mSlo* was mutated to a lysine residue (TTG), which allowed for the translation of nine additional bases (CTCCCAGGA) at the c-terminus of *mSlo* before the sequence of GFP began. As a result of the subcloning steps, fourteen base pairs were eliminated from the 3' untranslated sequence of *mSlo* (CTATTTTTTTAAAG). A mismatch mutagenesis strategy (Kammann et al., 1989) using PCR (polymerase chain reaction) was employed to produce the mutations of the stop codon and subcloning. DNA fragments were separated by agarose gel electrophoresis and purified using QIAQUICK gel extraction kit (Qiagen, Chatsworth, CA). Oligonucleotides used in this study were custom made by the Oligonucleotide Core Facility at the University of Rochester. To confirm the fusion construct, DNA sequencing was carried out at the Oligonucleotide Core

Facility using the dideoxy chain termination method (Sanger et al., 1977).

Whole cell and vesicle preparation

COS-7 cells (ATCC, Rockville, MD) were incubated in a CO_2 incubator in 100 mM tissue culture plates at 37 °C until they reached 70-80% confluency. The cells were then transfected using a DEAE-Dextran cationic-lipid method (Oprian et al., 1987) using 2 µg of DNA per plate. Cells were assayed for channel activity by patch clamp or harvested into vesicles for reconstitution into lipid bilayers 48 to 72 hours after transfection. For lipid bilayer preparation, the cells were scraped off the culture plates and collected into ice cold 10 mM sodium phosphate buffer, pH 7.0, containing 150 mM NaCl. The cells were resuspended in a high pH solution (150 mM KCl, 2mM $MgCl_2$, 5 mM EGTA, pH 10.6 with ammonium hydroxide) and broken up by being taken up in a 20 ml syringe 4 times through a high gauge needle (2 times with a 22 gauge, then 2 times with a 25 gauge). The broken cells were sonicated 30 secs to form lipid vesicles (Branson model 450 sonicator, duty cycle 50%, output 4). The vesicles were purified on a step sucrose gradient (40% and 20% sucrose cushion, interface between these layers contains the vesicles). The purified vesicles containing the channels were resuspended in isotonic sucrose buffer (10 mM MOPS and 250 mM sucrose, pH 7.4), quick frozen on dry ice, and stored at -80°C.

Electrophysiology

For single channel analysis, the vesicles containing the recombinant channels were reconstituted into lipid bilayers and characterized. The recording chamber was made out of acetyl copolymer (Patriot Plastics, Londonderry, NH). It includes two open wells (one with a glass side called the *cis* chamber and another behind it called the *trans* chamber) separated by a thin wall with a 250 µm hole drilled through it. A forming solution of 100 µl of N_2 dried lipid (1-palmitoyl, 2-oleoyl-phosphotidylethanolamine/1-palmitoyl, 2-oleoyl-phosphotidylcholine, 10 mg/ml, (Avanti Polar Lipid, Alabaster, Al), 7:3 respectively and 50 µl *n*-decane (Sigma) was used to prepaint the chamber. The *cis* chamber contained 650 mM KCl, 10 mM HEPES, 100 µM Ca^{2+}, pH 7.4. The *trans* chamber contained an identical solution, except its KCl concentration was 50 mM. Vesicles from the COS cell prep were added to the *cis* chamber and after incorporation of a single maxi-K channel, the *cis* side of the chamber was perfused with 150 mM KCl and KCl was added to the *trans* chamber resulting in an isotonic KCl concentration of 150 mM for all recordings. To measure calcium activation and sensitivity to block, stock solutions of $CaCl_2$, $BaCl_2$, and recombinant CTX were pipetted into the appropriate chamber when needed. The CTX used was purified to its active form after cleavage from a fusion protein in *E. Coli* (Park et al., 1991). The *trans* chamber was connected to ground and all the voltages in the *cis* chamber are expressed relative to ground. The CTX experiments were all carried out at + 30 mV.

For patch clamp experiments, whole cell currents were evoked by voltage steps from -50 mV to +30 mV (with a holding potential of -80 mV), and single channel currents evoked in excised inside out patches at a holding potential of +40 mV. The extracellular solution consisted of (in mM): 140 NaCl, 2.8 KCl, 1.0 $MgCl_2$, 10 HEPES, 10 glucose, pH 7.4 with 100 µM $CaCl_2$, and the pipet solution consisted of (in mM): 140 KCl, 2 $MgCl_2$, 1.1 EGTA, 0.1 $CaCl_2$, 5 HEPES, and 5 K_2-ATP.

Data acquisition and analysis

The *cis* and *trans* chambers were connected with electrodes to an Axopatch 200A patch clamp amplifier (Axon Instruments, Foster City, CA) in capacitive feedback configuration. The lowpass cutoff filtering frequency was set at 1 kHz. The analog output signal was digitized by a Data Acquisition Processor (DAP) 3200e, (Microstar Laboratories) at 100 kHz. Open and closed times were computed by an on-board processor (486DX) on-line at 100 kHz with a threshold set at 50% of the whole open-level current. At the same time, single-channel currents were sampled at 1 kHz. Cumulative open probability (P_o) was computed from the total open and closed times. During the recording, P_o *vs.* number of transitions was displayed after every 1,000 transitions. Patch Clamp data were also obtained using an Axopatch 200 amplifier (5 kHz low pass filter) and currents were recorded using pCLAMP 5.2 software. Rate constants for association and dissociation of CTX and Ba^{2+} were calculated from the statistical distributions of the blocked and unblocked dwell times, as previously described (Anderson et al., 1988). A pentium/150 MHz Personal Computer and a custom written program were employed to control the experiment, and to store and analyze the data.

Detection of expressed fluorescence

The cells were imaged for analysis in one of two ways: 1) To obtain higher resolution in imaging the fusion construct, the cells were fixed in 4% paraformaldehyde and washed in 0.05 M phosphate buffer. The cells were air dried and mounted for observation on a Nikon microphot fluorescence microscope (figure 1). All cells were imaged using a Hoffman Modulated contrast objective. The cells were excited with UV light (mercury lamp), and observed in the green wavelength (with a Fitc filter cube). 2) Similar results were obtained using confocal microscopy (data not shown) at the Adherent Cell Analysis and Sorting (ACAS) Facility of the University of Rochester. They were trypsinized and transferred to quartz plates for imaging. The cells were excited at a wavelength of 395 nm and their relative fluorescence was recorded at 488 nm.

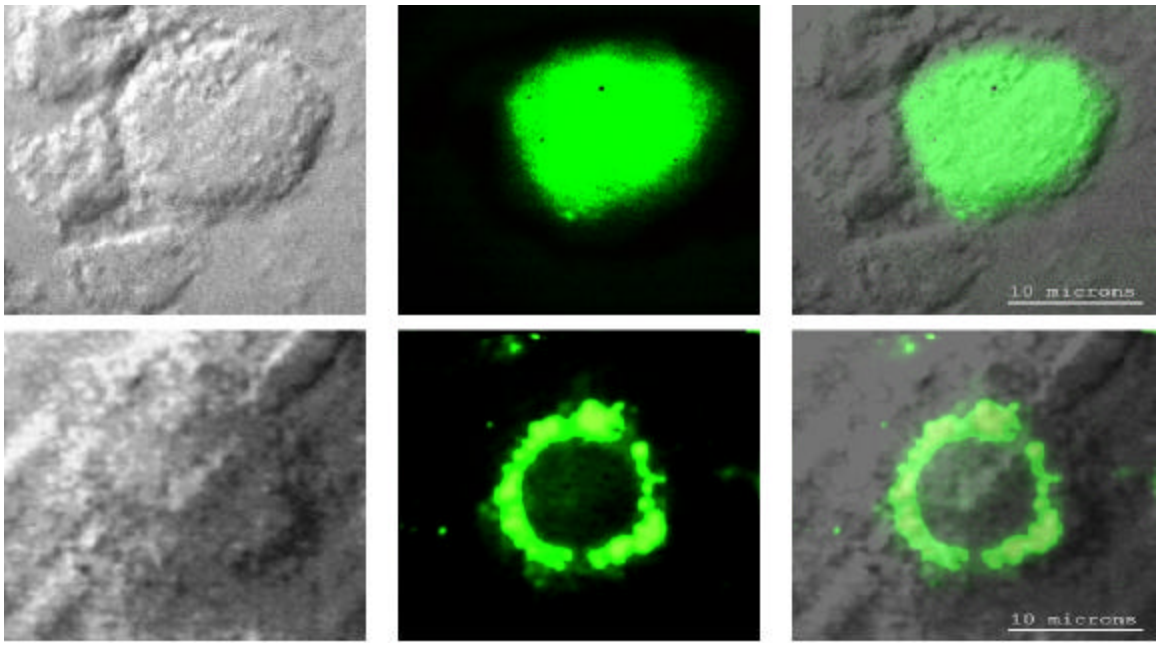

Figure 1. COS-7 cells transfected with Green Fluorescent Protein (GFP) and the *mSlo*-GFP fusion protein.

Top panels: Section of COS-7 cells transfected with GFP-pMT3 showing one cell with intense fluorescence. The left panel is a bright field image of the cells, the middle panel is a pseudo color image of the relative level of fluorescence, the right panel is a layered image of the first two panels, with scale bar (all images created on the same page in Adobe Photoshop). Bottom panels: Section of COS-7 cells transfected with *mSlo*-GFP-pMT3 showing one cell with intense localized fluorescence. Panels are the same as above (note a cell process from another cell in the upper right corner).

Results

Visualization of GFP and expressed channels

To find the optimal conditions for transfection, the fusion protein was used to transfect COS-7 cells under differing conditions of cell density, concentrations of DNA to lipid reagent, and transfection times. When GFP was expressed alone in our cloning vehicle (plasmid vector GFP-pMT3), conventional fluorescent microscopy revealed cells labeled with intense fluorescence throughout the cell (figure 1, top panels). When GFP was fused to the maxi-K channel (plasmid vector *mSlo*-GFP-pMT3), the same microscopy revealed robust fluorescence localized near the cell membrane (figure 1, bottom panels). After transfection with *mSlo*-GFP-pMT3, fluorescent cells that were patch-clamped (4 out of 5), displayed typical outward going voltage gated maxi-K currents (figure 2, A and B). COS-7 cells that were not fluorescing showed no currents (4 out of 4).

Characterization of channels reconstituted into lipid bilayers

Currents through *mSlo* channels reconstituted into lipid bilayers had an average conductance of 265 pS and were voltage dependent (figure 3, A and B). The opening of the tagged channel was also voltage dependent with an average channel conductance of 272 pS (figure 3, D and E). *mSlo* was calcium sensitive in the μM range (figure 3C), which closely matches the calcium sensitivity of *mSlo*-GFP (figure 3F). The calcium activation data was least-squares fitted with the Hill equation (K_D = 13.9 μM, n = 2.9, V_{max} = 94, and K_D = 11.2 μM, n = 2.5, V_{max} = 84 for *mSlo* and *mSlo*-GFP, respectively). Although only one distribution of the voltage dependence is displayed for typical *mSlo* and *mSlo*-GFP channels, both the calcium and voltage sensitivity varied from channel to channel. Wu et al. (1996), describe the calcium variation as a clustered distribution of calcium sensitivities in maxi-K channels from avian nasal gland cells. To determine any differences in voltage or calcium sensitivity, the open probability of several single channel experiments under identical conditions of voltage and free calcium concentration were averaged together. The mean open probabilities of *mSlo* and *mSlo*-GFP channels (63.9 ± 4.5% and 52.8 ± 12%, n = 10 and 9, respectively) were not significantly from each other at +30 mV and 100 μM Ca^{2+}. Thus, the addition of green fluorescent protein to the *mSlo* channel had very little, if any, effect on its functional characteristics described above.

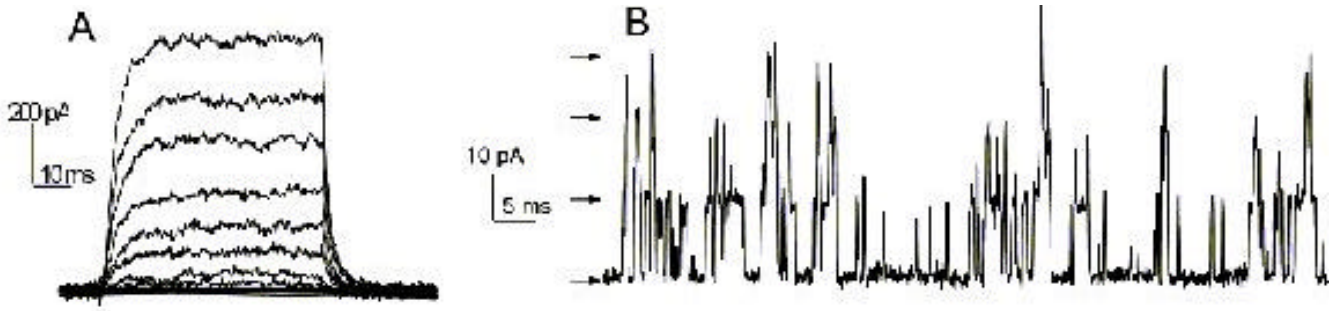

Figure 2. Currents recorded from a fluorescing COS-7 cell transfected with *mSlo*-GFP-pMT3

A: Whole cell currents were evoked by voltage steps from -50 mV to +30 mV (with a holding potential of -80 mV). The extracellular solution consisted of (in mM): 140 NaCl, 2.8 KCl, 1.0 $MgCl_2$, 10 HEPES, 10 glucose, pH 7.4 with 100 μM $CaCl_2$, and the pipet solution consisted of (in mM): 140 KCl, 2 $MgCl_2$, 1.1 EGTA, 0.1 $CaCl_2$, 5 HEPES, and 5 K_2-ATP. **B**: Multiple single channel currents (arrows denote each channel level) recorded from an excised inside out patch of a fluorescing COS-7 cell. Currents of about 16 pA were evoked (solutions were the same as above, with a holding potential of +40 mV).

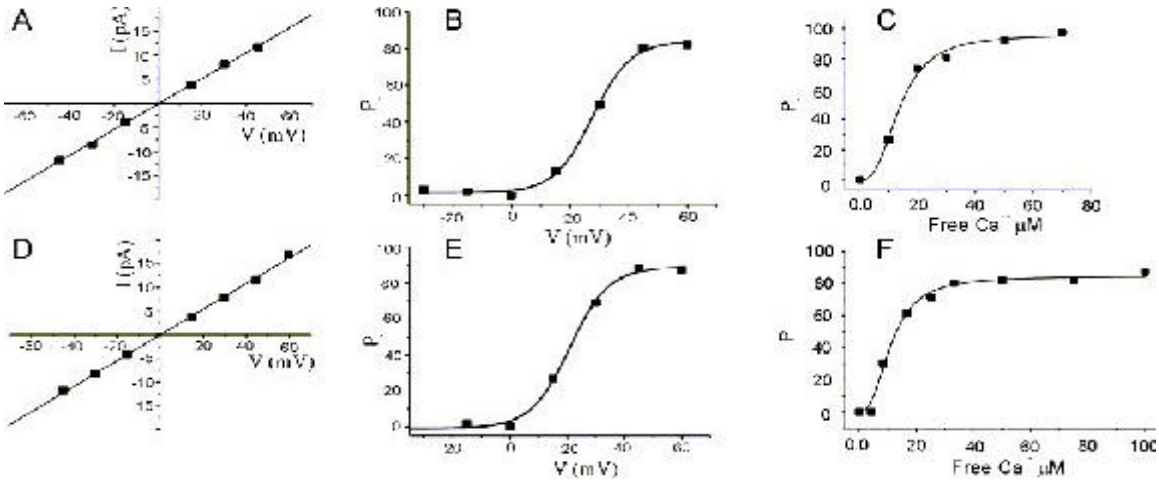

Figure 3. Currents through *mSlo* and *mSlo*-GFP channels from transfected COS-7 cell membranes reconstituted into lipid bilyers.

A: The current-voltage relationship of *mSlo* channels, with the solid line representing a linear fit of 8 single channel experiments (n=5 for each data point). The standard error of the mean (SEM) is less than the width of the points and the average channel conductance was 265 pS. **B**: Voltage dependence of a typical single *mSlo* channel. The solid line represents a least squares fit of the Boltzman distribution. **C**: Single channel current (*mSlo*) activation by free Calcium added to the internal side of the channel in 150 mM symmetrical KCl. The data was least-squares fitted with the Hill equation (K_D = 13.9 μM, n = 2.9, V_{max} = 94). **D**: The current-voltage relationship of *mSlo*-GFP channels, with the solid line representing a linear fit of 9 single channel experiments (n=5 for each data point, except for +60 mV, where n =1). The standard error of the mean (SEM) is less than the width of the points and the average channel conductance was 272 pS. **E**: Voltage dependence of a single *mSlo*-GFP channel in 150 mM symmetrical KCl. The solid line represents a least squares fit of the Boltzman distribution. **F**: Single channel current (*mSlo*-GFP) activation by free Calcium added to the internal side of the channel in 150 mM symmetrical KCl. The data was least-squares fitted with the Hill equation (K_D = 11.2 μM, n = 2.5, V_{max} = 84).

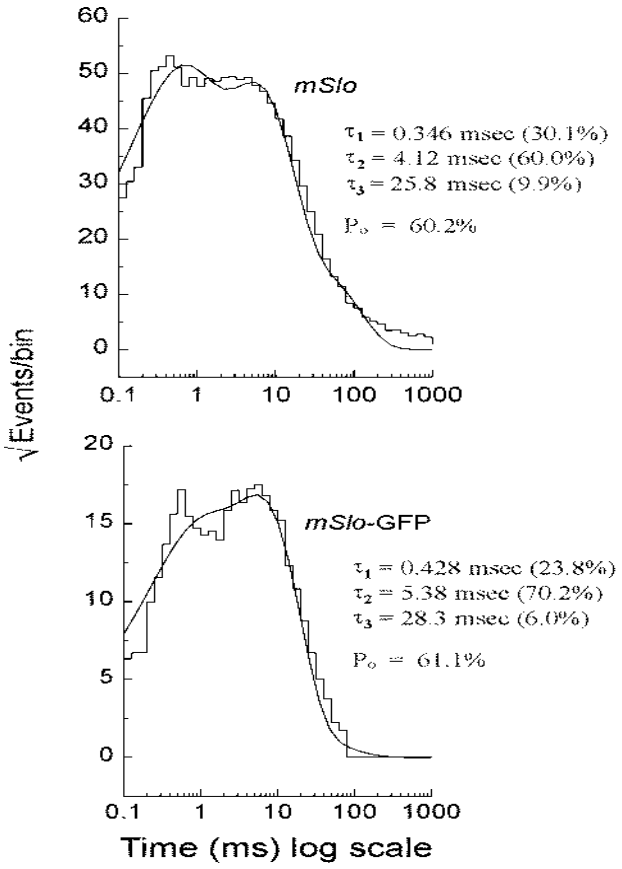

Figure 4. Closed dwell time histograms of *mSlo* and *mSlo*-GFP

The top histogram shows the distribution of 23,500 shut times in a control experiment with no CTX added to the external side of the channel *mSlo*. The bottom histogram shows the distribution of 22,500 shut times in a control experiment with no CTX added to the external side of the channel *mSlo*-GFP. The histogram data were overlayed with the probability density function.

Statistical distribution of *mSlo* and *mSlo*-GFP dwell times

To further test if the gating of the channel was unchanged, the statistical distributions of the shut and open times of control records were analyzed using the probability density function (representative distributions of shut and open dwell times are shown in figures 4 and 5. respectively). Rate constants from 4 channels for each clone with similar open probabilities were averaged together (see table 1). We were able to resolve 3 exponents to describe the distribution of the shut times of the channels. The average shut time rate constants ± SEM, were: τ_{c1} = 0.453 msec ± 0.103, τ_{c2} = 4.30 msec ± 0.540, τ_{c3} = 19.1 msec ± 2.95 for *mSlo*, and τ_{c1} = 0.544 msec ± 0.101, τ_{c2} = 4.43 msec ± 0.962, τ_{c3} = 16.5 msec ± 2.95 for *mSlo*-GFP, respectively (see table 1). The distribution of the open dwell times were well described by a single exponent, 5.26 ± 0.923 msec for *mSlo*, and 6.07 ± 1.27 msec for *mSlo*-GFP (see table 1). These values are consistant with those recently reported for wild type *mSlo* (Sullivan et al., 1997). The rate constants describing the open and shut times of both channels were nearly identical for the wild type *mSlo* and *mSlo*-GFP fusion channels. Thus adding GFP to the channel does not appear to have any significant effect on the gating of the channel.

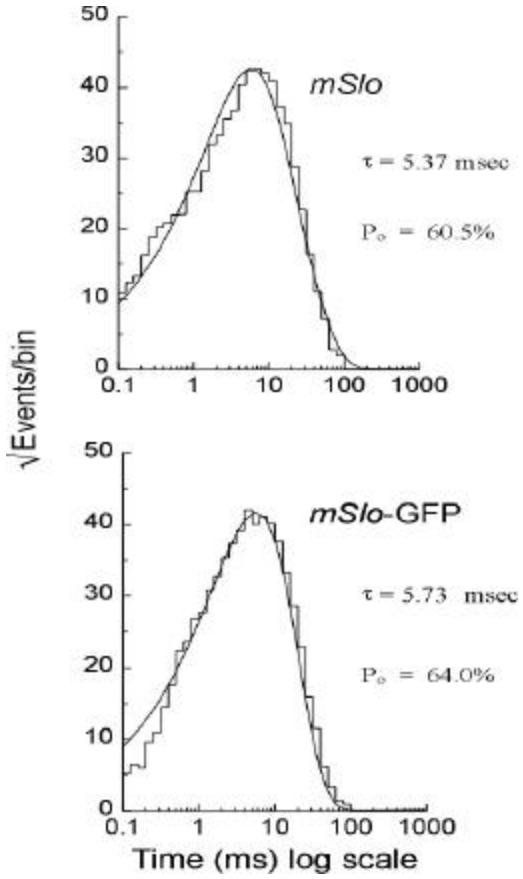

Figure 5. Open time histograms of *mSlo* and *mSlo*-GFP.

The top histogram shows the distribution of 23,500 open times in a control experiment with no CTX added to the external side of the channel *mSlo*. The bottom histogram shows the distribution of 10,500 open times in a control experiment with no CTX added to the external side of the channel *mSlo*-GFP. The histogram data were overlayed with the probability density function.

CTX block of *mSlo* and *mSlo*-GFP

Structural features of the *mSlo*-GFP fusion channel, namely the outer vestibule, were explored using CTX and Barium, respectively, as probes. CTX block of typical single channels (figure 6) revealed similar functioning of the two channels. The K_D for CTX block for the fused channel was 7.5 nM compared to 7.3 nM for *mSlo* (see table 2). Ba^{2+} was also used to probe the channels in a single experiment one ach clone (see figure 6). The Barium block of

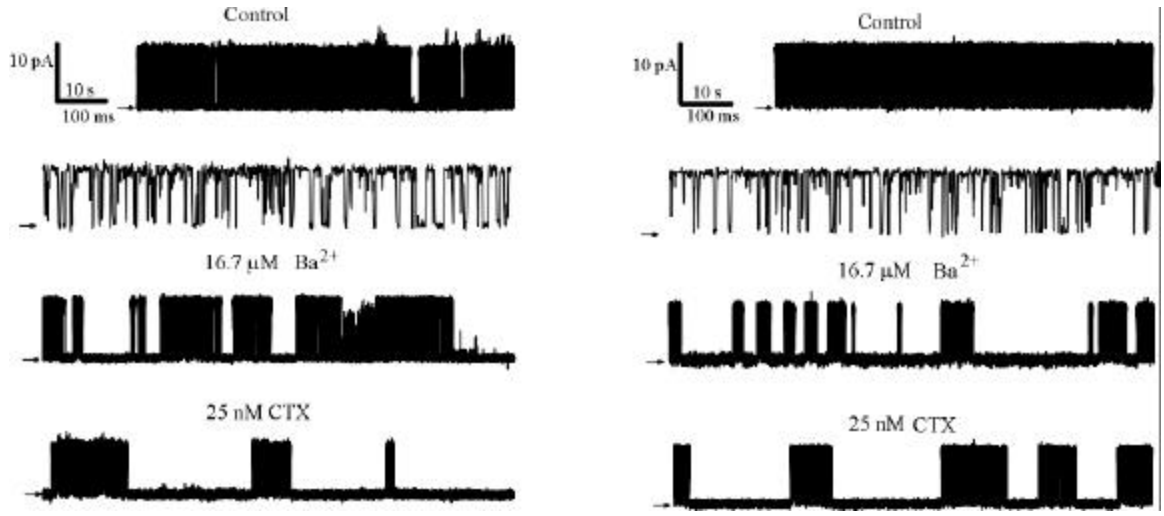

Figure 6. Single channel assay of *mSlo* (left traces) and *mSlo*-GFP (right traces) with Barium and charybdotoxin (CTX).

Channels were expressed in COS-7 cell membranes and incorporated into lipid bilayers. Channel openings are upward, and the small arrow to the left of each trace denotes the closed state. All traces represent single channel currents in symmetrical 150 mM solutions at +30 mV. Top traces represent control experiments with no CTX. An expanded time scale is shown in the Traces second from the top represent a portion of the trace above with a 100 fold expanded time scale. From 23 minutes of recorded data for CTX block of *mSlo*-GFP, the burst time constant was 3.12 sec and the blocked time constant was 13.1 sec, which corresponds to an on rate of 12.8 x 10^6 s^{-1} M^{-1} and an off rate of 76.3 x 10^{-3} s^{-1}, respectfully. These data give a CTX equilibrium constant K_D of 6.0 nM for this channel. These data closely match the single channel diplayed for *mSlo*, which has a CTX equilibrium constant K_D = 6.7 nM. For overall kinetic parameters from a total of 12 experiments, see table 1. The Barium block of m*Slo*-GFP shows a blocked time constant of 4.56 sec, almost exactly equal to m*Slo* (4.64 sec).

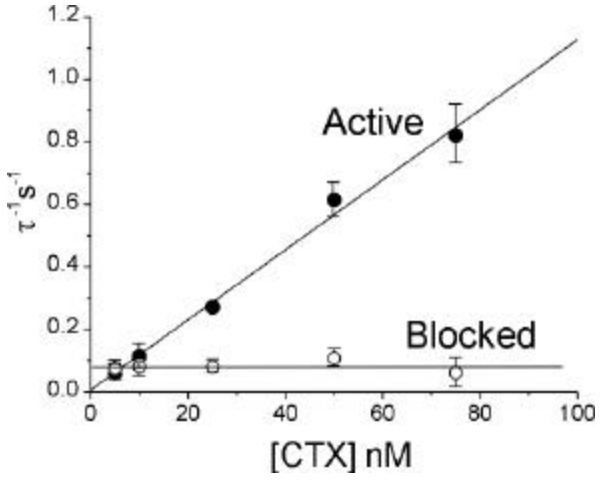

Figure 7. Concentration dependence of CTX Block of *mSlo*.

At each CTX concentration, records were taken for 25-45 min, and mean dwell times were calculated for the active (bursts, solid circles) state and the blocked (open circles) state. Each point represents the mean dwell time (± s.e.m.) calculated from 3 to 5 separate single channels. Each line represents a linear fit of the data. Note that the point at which the lines cross is equal to the K_D (7.4 nM for *mSlo*).

mSlo-GFP showed a blocked time constant of 4.56 sec, compared to a blocked time constant of 4.64 sec for *mSlo*.

Concentration dependence of CTX block of *mSlo*

To investigate the concentration dependence of CTX block of *mSlo*, the channel was assayed with the toxin at several different toxin concentrations (see figure 7). As seen with native maxi-K channels, the interaction of CTX with *mSlo* was bimolecular. The blocked dwell times were exponentially distributed and the average blocked time, τ_b, was independent of toxin concentration (figure 7, open circles). Increasing the concentration of CTX has no effect on the off rate. The burst times were also exponentially distributed and the on rate increased with increased toxin concentration (figure 7, closed circles). As the concentration of CTX was increased, the on rate increased linearly.

Discussion

We have used GFP to estimate expression of maxi-K channels prior to reconstitution into lipid bilayers and to locate transfected cells for patch clamping. The fusion protein has allowed us to monitor transfection conditions necessary to express the α subunit of *mSlo*. Given that single channel recordings of *mSlo* are rare (Muller et al., 1996) yet essential for a detailed evaluation of CTX block including its interaction with the subunit (Strobaek et al., 1996), a functional reporter gene to monitor expression in various expression systems and conditions is a powerful tool. In this study, we have demonstrated that the *mSlo* channel expression and protein targeting, kinetics, and functional properties of the outer vestibule are all unchanged by GFP fusion at the carboxy-terminus.

Our halo like location of the protein (figure 1, bottom panels) has also been seen in a preliminary report of another tagged potassium channel (John et al., 1997), and suggests that the channels are inserted into the plasma membrane. Therefore, sub-cellular localization of ion channels now appears possible. As expression of various constructs are undertaken to elucidate ion channel structure and function, it has been suggested that tagging of these clones will help us to distinguish between non-functional channels and those whose biogenesis was arrested (Makhina et al., 1997). Thus this new construct represents a tag to not only monitor channel expression, but to locate the protein in living cells. A preparation of transfected cells can now be checked for efficiency before they are reconstituted simply by evaluating the fluorescence of the cells. The fluorescence observed is quite stable, and we demonstrate here that cells with no fluorescence do not express channels. The patch clamp and lipid bilayer results, as well as the fluorescent images suggest that the GFP is indeed fused to the channel and that the channel is fully functional. Moreover, a functional delayed rectifier K^+ channel clone (RCK1) has recently been fused to GFP and characterized (Trouet et al., 1997), further demonstrating that GFP can mark cells while not affecting channel behavior.

Our analysis of the time constants and distributions for the *mSlo* and *mSlo*-GFP fusion channels revealed that the normal gating of the channel was apparently unaffected by addition of GFP to the c-terminus. Our time constants are consistent with those previously reported for *mSlo*. Sullivan et al. (1997), describe the open times with one exponent (τ_o = 58 msec), and were able to resolve 4 exponents to describe the shut times of *mSlo*: τ_{c1} = 0.59 msec, τ_{c2} = 2.5 msec, τ_{c3} = 9.4 msec, and τ_{c4} = 238 msec at +20 mV in 200 μM Ca^{2+}. Their experimental conditions (designed to analyze calcium sensitivity) were very different from ours, making a comparison difficult.

While attaching GFP to the carboxy-terminus of *mSlo* had no effect on channel function, results from an amino-terminus attachment to *hSlo* were quite different. Tagging the amino-terminus of *hSlo* with GFP apparently alters its calcium sensitivity (Meyer and Fromherz, 1999). No such affect on calcium sensitivity seen in our carboxy-terminus construct could be a clue that only the amino-terminus of the protein is involved in sensing calcium. A more detailed examination of the calcium sensitivity of our tagged protein will need to be done before a final conclusion can be made. The amino-terminus tagged *hSlo* result also suggests that care should be taken before extrapolating the results presented here to other channels.

Another result of this study has been a single channel look at the functional inhibition of CTX on the α subunit of *mSlo*. Our K_D value of 7.4 nM for *mSlo* and 7.6 nM for *mSlo*-GFP are on the order of the inhibition constant recently reported for the other CTX sensitive BK clone *hSlo* (Gribkoff et al., 1996). The EC_{50} for CTX of *hSlo* in the Gribkoff et al. study (estimated from inhibition of two-electrode voltage clamped current from oocytes) is 30.8 nM and 7.9 nM for Iberiotoxin (IbTX), a close structural homologue of CTX. The EC_{50} of IbTX (also estimated from inhibition of two-electrode voltage clamped current from oocytes) in *mSlo* was estimated to be 9.1 nM in the Gribkoff et al. (1996) study. In addition, we demonstrate here that CTX block of *mSlo* is bimolecular, showing that the clone follows the interaction of CTX with native maxi-K channels (Miller et al., 1985). The Gribkoff et al. (1996) study did not assess the concentration dependence of CTX block on *mSlo*. They did find a bimolecular interaction for IbTX with both *hSlo* and *mSlo* channels which corresponds to our finding. Their result of the interaction of CTX with *hSlo* was less definitive. A functional inhibition of CTX on *hSlo* single channel current may reveal a more detailed answer. The green fluorescent protein (GFP) from the jellyfish *Aequorea victoria* has become an important reporter molecule for monitoring gene expression. With this work, an RCK1 chimera (Trouet et al., 1997), and preliminary reports of other potassium channel GFP fusion

Table 1. Time constants and open probabilities of *mSlo* and *mSlo*-GFP channels

Channel type	τ_{c1} (msec)	τ_{c2} (msec)	τ_{c3} (msec)	τ_o (msec)	P_o (%)	n
mSlo	0.453 ± 0.103	4.30 ± 0.54	19.1 ± 2.9	5.26 ± 0.92	64.2 ± 2.1	4
mSlo-GFP	0.544 ± 0.101	4.43 ± 0.96	16.5 ± 4.4	6.07 ± 1.27	65.2 ± 2.0	4

Analysis of dwell time histograms (representative histograms are shown in figures 4 and 5) measured at + 30 mV in symmetrical 150 mM KCl and 100 μM Ca^{2+}. Closed time histograms were fitted with three exponentials (τ_{c1} - τ_{c3}), and open time histograms were fitted with one exponential (τ_o). Each value represents the mean ± SE of the number of measurements reported (*n*), each representing control recordings of a single channel in a separate bilayer.

Table 2. Kinetic parameters for CTX block of *mSlo* clones

Channel type	k_{off} ($x10^{-3}$ s^{-1})	k_{on} ($x10^{6}$ s^{-1} M^{-1})	K_D (nM)	n
mslo	74 ± 7	10 ± 0.6	7.4	7
mSlo-GFP	82 ± 14	11 ± 1.3	7.6	5
rat skeletal muscle*	62 ± 3	7.0 ± 1.1	8.8	9

Association and dissociation rate constants of CTX, k_{on} and k_{off}, and the dissociation constant K_D, were measured at + 30 mV on single maxi-K channels. Each value represents the mean ± SE of the number of measurements reported (*n*), each employing 100-246 blocking events of a single channel in a separate bilayer. *(Stampe et al., 1994)

proteins (John et al., 1997; Makhina et al., 1997; Veyna-Burke et al., 1997), as well as calcium channel GFP chimeras (Grabner et al., 1997; Zhou et al., 1997), a new list of GFP constructs will have to be added to the existing categories (Gerdes and Kaether, 1996), namely ion channels. Since we have demonstrated here that only fluorescent COS-7 cells express the clone, patch clamping only fluorescent oocytes should increase the chances of recording from BK clonesand not endogenous maxi-K channels. Although we have not expressed and imaged *mSlo*-GFP in *Xenopus laevis* oocytes in this study, a recent report of another GFP fused K^+ channel demonstrated that the fluorescent protein (constructed with the same fluorescent tag from Clontech, Palo Alto, CA) displayed surface expression in oocyte membranes resulting in visible fluorescence and macroscopic currents (Chan et al., 1997). Just as *mSlo*-GFP has allowed us to asses the affinity of CTX for *mSlo*, currents through GFP tagged G protein inwardly rectifying K^+ (GIRK) channels have recently identified specific regions of subunits involved in channel openings (Chan et al., 1997). Ion channels fused to GFP have limitless applications in studying the structure and function of these proteins. Our fluorescing protein represents a tagged maxi-K channel. The use of fluorescent *mSlo*-GFP will hopefully shed some light on the limited information we have about these critical proteins.

Acknowledgments

The authors would like to thank Lawrence Salkoff for the use of *mSlo*, Peter Shrager for the use of the Nikon fluorescent microscope, and Ted Begenisich for help in improving the manuscript. A special thanks goes to Ian Vabnick for help in recording the fluorescent images and for the support of the members of the Papazian Lab at UCLA.

References

Adelman, J.P., Shen, K.Z., Kavanaugh, M.P., Warren, R.A., Wu, Y.N., Lagrutta, A., Bond, C.T., and North, R.A. (1992). Calcium-activated potassium channels expressed from cloned complementary DNAs. Neuron, 9:209-216.

Anderson, C.S., MacKinnon, R., Smith, C., and Miller, C. (1988). Charybdotoxin block of single Ca^{2+}-activated K^+ channels. Effects of channel gating, voltage, and ionic strength. Journal of General Physiology, 91:317-333.

Asano, M., Nomura, Y., Ito, K., Uyama, Y., Imaizumi, Y., and Watanabe, M. (1995). Increased function of voltage-dependent Ca^{2+} channels and Ca^{2+}- activated K^+ channels in resting state of femoral arteries from spontaneously hypertensive rats at prehypertensive stage. Journal of Pharmacology and Experimental Therapeutics, 275:775-783.

Balwierczak, J.L., Krulan, C.M., Kim, H.S., DelGrande, D., Weiss, G.B., and Hu, S. (1995). Evidence that BKCa channel activation contributes to K^+ channel opener induced relaxation of the porcine coronary artery. Naunyn-Schmiedeberg's Archives of Pharmacology, 352:213-221.

Barnes, P.J. (1995). Molecular mechanisms of antiasthma therapy. Annals of Medicine, 27:531-535.

Bontems, F., C. Roumestand, P. Boyot, B. Gilquin, Y. Doljansky, A. Menez, and F. Toma. (1991). Three-dimensional structure of natural charybdotoxin in aqueous solution by 1H-NMR. Charybdotoxin possesses a structural motif found in other scorpion toxins. European Journal of Biochemistry, 19619-28.

Bringmann, A., Faude, F., and Reichenbach, A. (1997). Mammalian retinal glial (Muller) cells express large-conductance Ca^{2+}-activated K^+ channels that are modulated by Mg^{2+} and pH and activated by protein kinase A. GLIA, 19:311-323.

Butler, A., Tsunoda, S., McCobb, D.P., Wei, A., and Salkoff, L. (1993). mSlo, a complex mouse gene encoding "maxi" calcium-activated potassium channels. Science, 261:221-224.

Chan, K.W., Sui, J.L., Vivaudou, M., and Logothetis, D.E. (1997). Specific regions of heteromeric subunits involved in enhancement of G protein-gated K^+ channel activity. Journal of Biological Chemistry, 272:6548-6555.

Doyle.D.A., J. Morais Cabral, R.A. Pfuetzner, A. Kuo, J.M. Gulbis, S.L. Cohen, B.T. Chait, and R. MacKinnon. (1998). The Structure of the potassium channel: molecular basis of K+ conduction and selectivity. Science, 280:69-77.

Dworetzky, S.I., Trojnacki, J.T., and Gribkoff, V.K. (1994). Cloning and expression of a human large-conductance calcium- activated potassium channel. Brain Research, Molecular Brain Research, 189-193.

Ferrer, J., Wasson, J., Salkoff, L., and Permutt, M.A. (1996). Cloning of human pancreatic islet large conductance Ca^{2+}-activated K^+ channel (hSlo) cDNAs: evidence for high levels of expression in pancreatic islets and identification of a flanking genetic marker. Diabetologia, 39:891-898.

Gerdes, H.H., and Kaether, C. (1996). Green fluorescent protein: applications in cell biology. FEBS Letters, 389:44-47.

Goldstein, S.A., Pheasant, D.J., and Miller, C. (1994). The charybdotoxin receptor of a Shaker K^+ channel: peptide and channel residues mediating molecular recognition. Neuron, 12:1377-1388.

Grabner, M., Dirksen, R.T., Proenza, C., and Beam, K.G. (1997). Functional Expression of Green Fluorescent Protein (GFP) Fused to Voltage-Dependent Calcium Channels in Dysgenic Myotubules. Biophysical Journal, 72:A146(abstract).

Gribkoff, V.K., Lum-Ragan, J.T., Boissard, C.G., Post-Munson, D.J., Meanwell, N.A., Starrett, J.E., Jr., Kozlowski, E.S., Romine, J.L., Trojnacki, J.T., McKay, M.C., Zhong, J., and Dworetzky, S.I. (1996). Effects of channel modulators on cloned large-conductance calcium-activated potassium channels. Molecular Pharmacology, 50:206-217.

John, S.A., Goldhaber, J.I., Weiss, J.N., and Ribalet, B. (1997). Ion Channels Fused to Green Fluorescent Protein Are Expressed Normally and Retain Physiological Properties. Biophysical Journal, 72:A253(abstract).

Kammann, M., J. Laufs, J. Schell, and B. Gronenborn. (1989). Rapid insertional mutagenesis of DNA by polymerase chain reaction (PCR). Nucleic Acids Research, 17:5404.

Knaus, H.G., Eberhart, A., Koch, R.O., Munujos, P., Schmalhofer, W.A., Warmke, J.W., Kaczorowski, G.J., and Garcia, M.L. (1995). Characterization of tissue-expressed alpha subunits of the high conductance Ca^{2+}-activated K^+ channel. Journal of Biological Chemistry, 270:22434-22439.

Krause, J.D., Foster, C.D., and Reinhart, P.H. (1996). Xenopus laevis oocytes contain endogenous large conductance Ca^{2+}-activated K^+ channels. Neuropharmacology, 35:1017-1022.

Latorre, R., Oberhauser, A., Labarca, P., and Alvarez, O. (1989). Varieties of calcium-activated potassium channels. [Review]. Annual Review of Physiology, 51:385-399.

MacKinnon, R., S.L. Cohen, A. Kuo, A. Lee, and B.T. Chait. (1998) Structural conservation in prokaryotic and eukaryotic potassium channels. Science, 280:106-109.

Makhina, E.N., Sha, Q., and Nichols, C.G. (1997). Expression of Green Fluorescent Protein (GFP)-Tagged Inward Rectifier K^+ Channel. Biophysical Journal, 72:A253(abstract).

Marshall, J., Molloy, R., Moss, G.W., Howe, J.R., and Hughes, T.E. (1995). The jellyfish green fluorescent protein: a new tool for studying ion channel expression and function. Neuron, 14:211-215.

McCobb, D.P., Fowler, N.L., Featherstone, T., Lingle, C.J., Saito, M., Krause, J.E., and Salkoff, L. (1995). A human calcium-activated potassium channel gene expressed in vascular smooth muscle. American Journal of Physiology, 269:H767-77.

McManus, O.B. (1991). Calcium-activated potassium channels: regulation by calcium. Journal of Bioenergetics and Biomembranes, 23:537-560.

Meyer E., and Fromherz, P. (1999). Ca^{2+} activation of hSlo K^+ channel is suppressed by N-terminal GFP tag. European Journal of Neuroscience , 11:1105-8.

Miller, C. (1995). The charybdotoxin family of K^+ channel-blocking peptides. Neuron, 15:5-10.

Miller, C., Moczydlowski, E., Latorre, R., and Phillips, M. (1985). Charybdotoxin, a protein inhibitor of single Ca^{2+}-activated K^+ channels from mammalian skeletal muscle. Nature, 313:316-318.

Muller, M., Madan, D., and Levitan, I.B. (1996). State-dependent modulation of mSlo, a cloned calcium-dependent potassium channel. Neuropharmacology, 35:877-886.

Myers, M.P., Yang, J., and Stampe, P. (1997). Visualization and Functional Analysis of a Cloned Maxi K^+ Channel (mSlo) Fused to Green Fluorescent Protein (GFP). Biophysical Journal, 72:A352-A352(abstract).

Naini, A.A., Shimony, E., Kozlowski, E., Shaikh, T., Dang, W., and Miller, C. (1996). Interaction of Ca^{2+}- activated K^+ channels with refolded charybdotoxins mutated at a central interaction residue. Neuropharmacology, 35:915-921.

Oprian D.D., Molday R.S., Kaufman R.J., Khorana H.G. (1987). Expression of a synthetic bovine rhodopsin gene in monkey kidney cells. Proceedings of the National Academy of Sciences of the United States of America, 84:8874-8.

Park, C.S., Hausdorff, S.F., and Miller, C. (1991). Design, synthesis, and functional expression of a gene for charybdotoxin, a peptide blocker of K^+ channels. Proceedings of the National Academy of Sciences of the United States of America, 88:2046-2050.

Sambrook, J., Fritsch, E.F., and Maniatis, T. (1989). Molecular Cloning. Plainview: Cold Spring Harbor Laboratory Press.Sanger, F., Nicklen, S., and Coulson, A.R. (1977). DNA sequencing with chain-terminating inhibitors. Proceedings of the National Academy of Sciences of the United States of America, 74:5463-5467.

Stampe, P., Kolmakova-Partensky, L., and Miller, C. (1994). Intimations of K^+ channel structure from a complete functional map of the molecular surface of charybdotoxin. Biochemistry, 33:443-450.

Strobaek, D., Christophersen, P., Holm, N.R., Moldt, P., Ahring, P.K., Johansen, TE, and Olesen, S.P. (1996). Modulation of the Ca^{2+}-dependent K^+ channel, hslo, by the substituted diphenylurea NS 1608, paxilline and internal Ca^{2+}. Neuropharmacology, 35:903-914.

Stumpff, F., Strauss, O., Boxberger, M., and Wiederholt, M. (1997). Characterization of maxi-K-channels in bovine trabecular meshwork and their activation by cyclic guanosine monophosphate. Investigative Ophthalmology and Visual Science, 38:1883-1892.

Sullivan D.A., Holmqvist M.H., and Levitan I.B. (1997). Characterization of gating and peptide block of mSlo, a cloned calcium-dependent potassium channel. Journal of Neurophysiology, 78:2937-50.

Tagaya, E., Tamaoki, J., Chiyotani, A., Yamawaki, I., Takemura, H., and Konno, K. (1995). Regulation of airway cholinergic neurotransmission by Ca^{2+}-activated K^+ channel and Na^+-K^+ adenosinetriphosphatase. Experimental Lung Research, 21:683-694.

Trouet, D., Nilius, B., Voets, T., Droogmans, G., and Eggermont, J. (1997). Use of a bicistronic GFP-expression vector to characterise ion channels after transfection in mammalian cells. Pflugers Archiv - European Journal of Physiology, 434:632-638.

Tseng-Crank, J., Foster, C.D., Krause, J.D., Mertz, R., Godinot, N., DiChiara, T.J., and Reinhart, P.H. (1994). Cloning, expression, and distribution of functionally distinct Ca^{2+}-activated K^+ channel isoforms from human brain. Neuron, 13:1315-1330.

Veyna-Burke, N., Li, D., Takimoto, K., Hoyt, K., Watkins, S., and Levitan, E.S. (1997). Localization and Mobility of GFP-K^+ Channel Fusion Proteins. Biophysical Journal, 72:A351(abstract).

Wallner, M., Meera, P., Ottolia, M., Kaczorowski, G.J., Latorre, R., Garcia, M.L., Stefani, E., and Toro, L. (1995). Characterization of and modulation by a beta-subunit of a human maxi K Ca channel cloned from myometrium. Receptors and Channels, 3:185-199.

Wu, J.V., T.J. Shuttleworth, and P. Stampe. (1996). Clustered distribution of calcium sensitivities - an indication of hetero-tetrameric gating components in Ca^{2+}-

activated K^+ channels reconstituted from avian nasal gland cells. Journal of Membrane Biology, 154:275-282.

Zhou, J., Cribbs, L., Yi, J., Shirokov, E., Perez-Reyes, E., and Rios, E. (1997). Cloning of an L-Type Ca Channel Homolog from Frog Skeletal Muscle and Functional Expression of a Chimeric Channel. Biophysical Journal, 72:A146(abstract).

Address for Correspondence:
Michael P. Myers, Ph. D.
Department of Physiology
UCLA School of Medicine
Los Angeles, California 90095-1751